ELSEVIER

Catalysis Today 32 (1996) 205–213

CATALYSIS TODAY

Structural modelling of coprecipitated VTiO catalysts

L.E. Briand *, R.D. Bonetto, M.A. Sanchez, H.J. Thomas

Centro de Investigación y Desarrollo en Procesos Catalíticos-INDECA 47 No. 257, (1900) La Plata, Buenos Aires, Argentina

Abstract

A statistical study of the particle shape and size of pure V_2O_5 and TiO_2, and samples of coprecipitated V_2O_5–TiO_2 catalysts with different V/Ti ratios, has been performed. They were also characterized by XRD, EDAX, SEM and XPS. The results showed that pure vanadium pentoxide is compose by large square or needle-shaped particles, while pure titanium dioxide has small and rounded ones. VTiO samples presented an area and shape, depending on the V/Ti ratio.

These results and the spectroscopical characterization conducted to a particle model of the catalysts. Those VOTi samples with high V/Ti ratio would have large V_2O_5 crystals acting as support of a V/TiO_2 solid solution. In contrast, those samples with a low V/Ti ratio, would have the solid solution supporting vanadium pentoxide crystals.

Keywords: V_2O_5; TiO_2; VTiO; Particle area; Shape factor; Characterization

1. Introduction

It is well known that selective oxidation of several substances are structure-sensitive to V_2O_5 and vanadium supported catalysts [1]. However, the structure-sensitivity of partial oxidation of hydrocarbons on coprecipitated VTiO catalysts has not been demonstrated yet, so, in the first place, it is necessary to perform a detailed characterization of the catalyst to model its particles. Depending on the V/Ti atomic ratio and the preparation procedure, different phases have been reported for VTiO catalysts, namely pure TiO_2 anatase, pure TiO_2 rutile, V_2O_5, lower V oxides, substitutional solid-state solution of V^{4+} in rutile and anatase, etc. [2–6]. All these species seem to play a definite role in the catalytic activity [1,7–9].

On the subject of coprecipitated VTiO catalysts, the study of Slinkard et al. [10] has shown that the solids VTiO, prepared either from an acid solution with base or a mixture of vanadyl and titanium oxalates, contained V_2O_5, TiO_2–rutile, TiO_2–anatase and a solid solution of V(IV) in TiO_2. Busca et al. [11] prepared solids by coprecipitation of $VOCl_3$ and $TiCl_4$ followed by calcination at 700°C and also identified a solution of V(IV) in anatase. Subsequent spectroscopical characterizations of these solids evidenced monooxovanadyl species on the surface [5].

Cavani et al. [12] have investigated the phases in solids VTiO that were prepared by several methods (flash drying, coprecipitation, wet impregnation, grafting). In all solids, they found that, besides crystalline V_2O_5, there were species V(V) and V(IV) strongly interacting with the

* Corresponding author. Tel.: 54 021 211353/210711. Fax: 54 021 254277.

PII S0920-5861(96)00188-5

titanium surface, and species V(V) in weak interaction. They also found that the preparation method strongly influences the concentration of the species; for instance, in coprecipitated oxides, they observed, for strongly interacting vanadium, that its concentration was higher than in those samples arrived at by impregnation of vanadium on titanium. Subsequent studies from the same authors have demonstrated that, from a mixture of solutions with complexes of both vanadium(IV) and titanium(IV), the precipitation produced solids with high vanadium oxide concentration, being this oxide in strong interaction with the titanium oxide. They also found that the presence of TiO_2, either anatase or rutile, did not influence the proportion of the different vanadium species [6].

More recently, Centi et al. [13] reviewed the structure of active sites in supported catalysts, and their relationship with catalytic activity with focus on V-oxide on TiO_2. The different preparation methods of systems of two oxides in contact, called by these authors "oxide-on-oxide systems", are: (i) wet impregnation with inorganic or organic salts, (ii) grafting, (iii) co-precipitation, (iv) sol-gel techniques, (v) solid-state reaction, and (vi) ion exchange. The preparation method mainly affects the initial dispersion of the active oxide on the other oxide, and not necessarily the characteristics and degree of interaction with the support. The dispersion of the active phase is an important factor in the catalytic activity because every reaction requires a specific dispersion; for instance, the alkane oxidative dehydrogenation requires stable isolated sites of vanadium whereas the oxidation of o-xylene to phthalic anhydride is catalyzed by solids containing a monolayer of vanadium-oxide on TiO_2. As a conclusion, different vanadium species, each with a particular catalytic behaviour, may be stabilized on an oxide support surface depending on the preparation method [14].

From the above paragraphs, it is evident that a detailed knowledge of the species and their distribution on the catalyst surface is important to understand the species and mechanisms involved in catalytic reactions. Therefore, in the present work, we performed a statistical study of the shape and size of coprecipitated VTiO catalysts, and pure phases V_2O_5 and TiO_2 anatase and rutile. The data so derived was combined to XRD, EDAX and XPS analysis to propose a model of the particle.

2. Experimental

2.1. Sample synthesis and characterization

The pure phases V_2O_5 and TiO_2–anatase were synthesized by precipitation in basic medium from $VOCl_3$ and $TiOCl_2$, respectively, and the TiO_2–rutile was obtained by calcination of anatase. These preparations were described in previous works [15,16].

Five samples of V_2O_5–TiO_2 with titanium percentages ranging from 10 to 90% were synthesized, and termed VT10, VT20, VT50, VT80, and VT90, respectively. All of them were obtained from $VOCl_3$ solutions, prepared by dissolving NH_4VO_3 (Mallinckrodt AR) in concentrated HCl (Merck PA), and $TiOCl_2$, also prepared just before use by hydrolysis of $TiCl_4$ (Carlo Erba RPE). These solutions were mixed in the appropriate proportions and neutralized in one step to pH 6 with NH_4OH (Merck PA) under continuous stirring and cooling. The precipitate was filtered and then washed with water to eliminate the NH_4Cl formed in the neutralization step. The solids so obtained were dried at 120°C and then calcined at 500°C for 96 h. In all thermal treatments, we employed either quartz or platinum laboratory materials to avoid bronze formation.

The catalysts were analyzed by EDAX, XRD, SEM and XPS. The equipment used and the sample preparation method was previously described [15,16]. To calculate the width at mid-height (FWHM) of plane (001) of phase V_2O_5, the X-ray diffraction signal was digitized as described in a previous work [16].

2.2. Scanning electron microscopy and image digitization. Data treatment

Images of the characteristic particles of the catalysts and of the pure phases were obtained by a Philips SEM 505 scanning electron microscope. To obtain good particle dispersion and a marked contrast between the particles and the sample holder, the samples were suspended in an aqueous medium with a concentration of 100 ppm, placed on cover glasses previously metalled with gold, dried and then metalled again. In order to convert the microscope images into useful mathematical information, we used an acquisition, processing and image analysis system specifically developed to work on images of the previously-described microscope [17]. The system consists of the following components:

(a) A device to digitally control the electron beam.

(b) A high frequency (1 MHz) analog–digital converter, which digitizes the signal sent to the photograph monitor of the microscope. Despite being a 12 bit converter that implies an input voltage that would convert into 4096 grey levels, the images were discretized in 8 bits (256 colours), which is enough for these type of images, thus avoiding memory problems.

(c) A Pascal program driving the communication between the electron beam controller and the computer to obtain both the digitized images and subsequent processing. To minimize the electronic noise when obtaining the images, we took an average of 16 measurements in each position of the electron beam. The program makes possible to obtain an histogram of the grey levels of the image, and to perform the image processing with the commoner filters: spatial, smoothing, thresholding, unsharp masking, roberts, sobel. The last three are used to reinforce the edges. The images are stored in bitmap file format (maximum size 1024×1024 pixels) so that they can be processed with any other commercial software for image processing.

(d) Programs to obtain the coordinates of the profile of digitized particles (the images of which were processed until a black and white image is created), and to characterize such particles according to their shape and size. This last program outputs histograms of distribution of particle areas, perimeters and shapes as well as the center of mass coordinates in each particle.

Histograms to be presented in the next sections were built by processing one hundred particles and are described with the mean values and standard deviations on Table 1.

Table 1
Mean area and shape factor of V_2O_5, anatase, rutile, and VTiO solids

Sample	Mean area (μm^2)	Mean S. factor
V_2O_5	104 ± 10	0.529 ± 0.012
TiO_2 anatase	0.153 ± 0.019	0.801 ± 0.079
TiO_2 rutile	0.354 ± 0.029	0.751 ± 0.009
VT10	13.6 ± 2.9	0.566 ± 0.010
VT20	4.45 ± 0.66	0.621 ± 0.017
VT50	5.79 ± 1.47	0.651 ± 0.012
VT80	0.049 ± 0.045	0.711 ± 0.013
VT90	0.105 ± 0.007	0.701 ± 0.013

3. Results and discussion

3.1. Catalysts characterization

Table 2 shows the mass analysis results of vanadium and titanium concentrations (expressed as $V/(V + Ti)$ and % of V_2O_5) measured by EDAX. The table also includes the surface concentration of such elements calcu-

Table 2
Surface and bulk analysis of VTiO catalysts

Sample	V/(V+Ti)		Vanadium pentoxide		% W/W TiO_2	
	bulk	surface	% W/W	FWHM	anatase	rutile
V_2O_5	1.00	1.00	100	0.19	—	—
VT10	0.89	0.82	9.9	0.17	23	77
VT20	0.86	0.84	87.0	0.17	10	90
VT50	0.56	0.37	57.6	0.18	90	10
VT80	0.27	0.38	27.9	0.16	92	8
VT90	0.13	0.28	14.2	0.17	38	62

lated with XPS results and the percentages of TiO_2 anatase and rutile, yielded by the equation of Seiyama et al., supplied with XRD analysis data [18]. FWHM values of the height of the signal $2\theta = 20.3°$ of plane (001) of vanadium pentoxide, are also shown.

Formerly, it was established that all samples VTiO are composed of well crystallized phases of V_2O_5 and TiO_2, being the latter found in anatase as well as in rutile varieties [15]. The cell volumes of these phases differ from those of pure anatase and rutile because of which it

Fig. 1. Comparison of intensities of X-ray reflections (001) and (200) of the vanadium pentoxide phase in the following samples: (A) VT10, (B) VT20, (C)VT50, (D) VT80 and (E) VT90. Symbols: (a) plane (001), (b) plane (200).

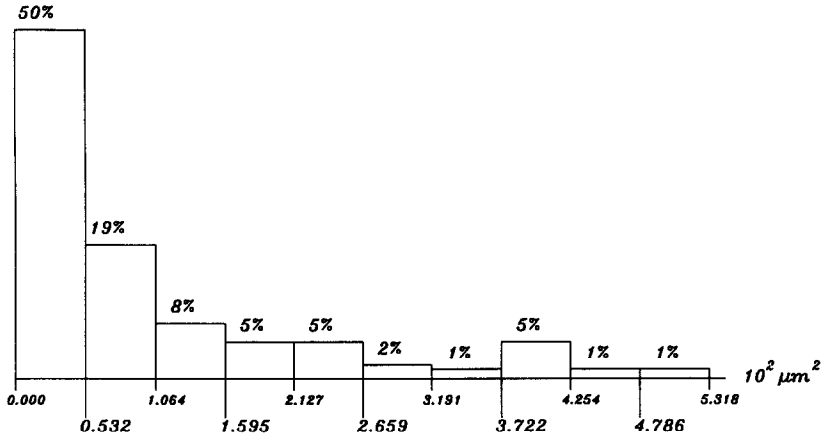

Fig. 2. Histogram of area distribution in pure V_2O_5 phase.

was found that the samples present solid solutions of vanadium which are of the substitutional type in anatase and of the interstitial type in rutile [16].

FWHM values in the plane (001) of vanadium pentoxide indicates that the vanadium phase crystallizes in the form of large crystals in all samples VTiO, regardless of the V/(V + Ti) ratio. Fig. 1 shows the X-ray diffraction signals of planes (001) and (200) of the vanadium pentoxide phase. Although the intensities of these signals may be changed by preferential orientation (a well known feature) when preparing the sample for the analysis, we observed that the intensities order $I(001) > I(200)$ was not altered after successive preparations and analysis of the solids.

In samples VT80 and VT90, the surface analysis revealed that the surface vanadium percentage is higher than its bulk concentration whereas in catalysts VT10, VT20 and VT50, the situation is opposite. In addition, a more exhaustive study of the surface was carried out by removing the crystalline vanadium pentoxide from the surface with a washing with concentrated ammonium hydroxide. The FTIR and laser Raman spectroscopy of the resultant solid permitted us to find a monolayer of species VOx strongly attached to the titanium which is similar to those previously encountered by other authors

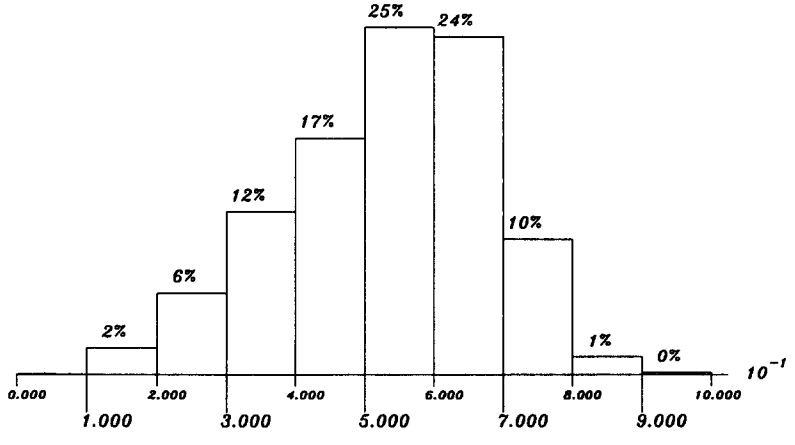

Fig. 3. Histogram of shape factor distribution in pure V_2O_5 phase.

on the surface of catalysts prepared by vanadium impregnation on TiO_2 [2,16,19,20].

3.2. Statistical study of particles by electron microscopy

As a shape parameter of the particles, we used a shape factor calculated by:

$$F = 4\pi \text{ area } (\text{perimeter})^{-2}. \quad (1)$$

This shape factor is not alter by rotation, scale and translation transformations. Furthermore, it describes the elongation of a particle shape, being maximum in a perfect circle and smaller for elongated shapes.

Fig. 2 and Fig. 3 present the distribution histograms for areas and shapes respectively, for the particles of the pure V_2O_5 phase. Most particle areas are within the 0–106.4 μm^2 and their shape factor range is 0.40–0.70. Table 1 displays the mean values and standard deviations of the area and shape parameters. As observed in Fig. 4, these values indicate that the vanadium pentoxide particles are mostly rectangular so that the shape factor already presented by Eq. (1) can be expressed now as:

$$F = \pi\alpha(\alpha + 1)^{-2}, \quad (2)$$

where $\alpha = b/a$; $\alpha > 1$, being a, b the rectangle sides.

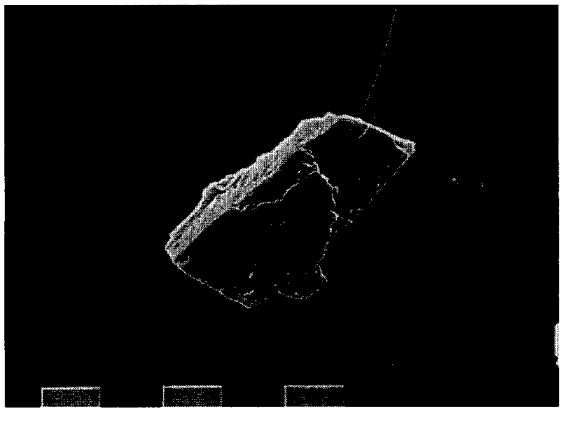

Fig. 4. Particle of pure V_2O_5 phase (x 1310).

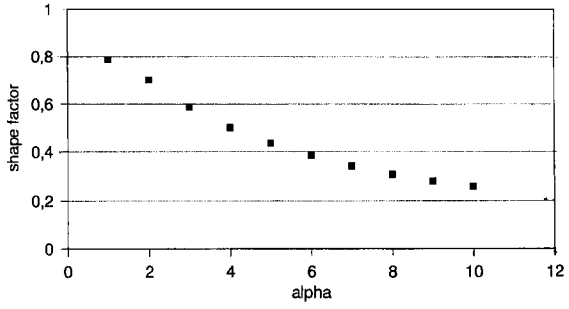

Fig. 5. Shape factor distribution as a function of the a/b ratio in V_2O_5.

Fig. 5 shows the values that would adopt the shape factor for different ratios a/b. The V_2O_5 presents a distribution varying from square-shaped particles (for which $a = b$) and $F =$ 0.785 to needle-shaped ones (where $b \gg a$ and $F = 0.098$).

Table 1 shows the mean values of the area and shape factor of pure TiO_2–anatase. Unlike the previous phase, the particles making up anatase are mainly of a considerably smaller size (0.153 ± 0.019 μm^2) than those of vanadium pentoxide. Particles shape is almost spherical, though the fact that they are not a perfect circle is reflected in their increased perimeter and, hence, in a decreased shape factor with mean values lower than 1 (0.801 ± 0.079).

In the rutile phase, shapes and areas of the particles (Table 1) are similar to those of the previous one. The particle areas of TiO_2 measured here coincide with literature values of the commercial oxides so we can ensure that, in our analysis, the contribution of particle agglomerates has been minimized [21–23].

With regard to solids VTiO, although the particle sizes of samples VT10 and VT20 (Table 1) are smaller than pure vanadium pentoxide, they show shape factors (0.566 ± 0.010 and 0.621 ± 0.017, respectively) which are typical of the morphology of that phase (Fig. 6). Unlike such samples, the particles of samples VT50, VT80 and VT90 are even smaller and round, which are typical of the titanium dioxide (Table 1, Fig. 7).

3.3. Particle modelling in coprecipitated catalysts VTiO

The particle morphology of these catalysts can be due to the order in which phases V_2O_5 and TiO_2 precipitate. In samples VT10 and VT20, the concentration of vanadium is higher than that of titanium so, during preparation, intermediate compounds precipitate first (oxichlorides, hydroxichlorides, hydroxides, oxides, etc.) which, by thermal decomposition generate vanadium pentoxide which, in turn, imparts its attributes of particle size and rectangular shape to the catalyst particles. Unlike these samples, catalysts VT50, VT80 and VT90 possess small and round particles; this is logical because, for these samples, the species leading to titanium dioxide by thermal decomposition

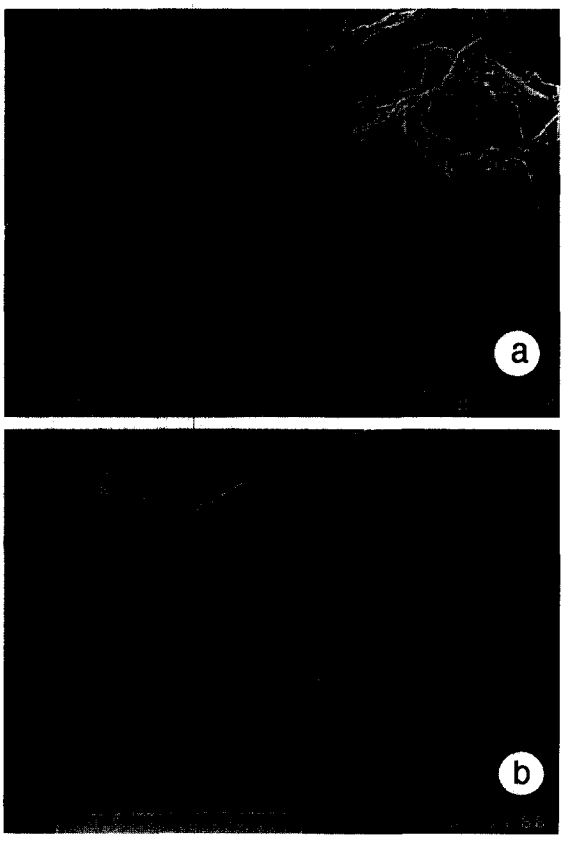

Fig. 6. (a) Morphology of VT10 catalyst (x 2000). (b) Isolated particle (x 5450).

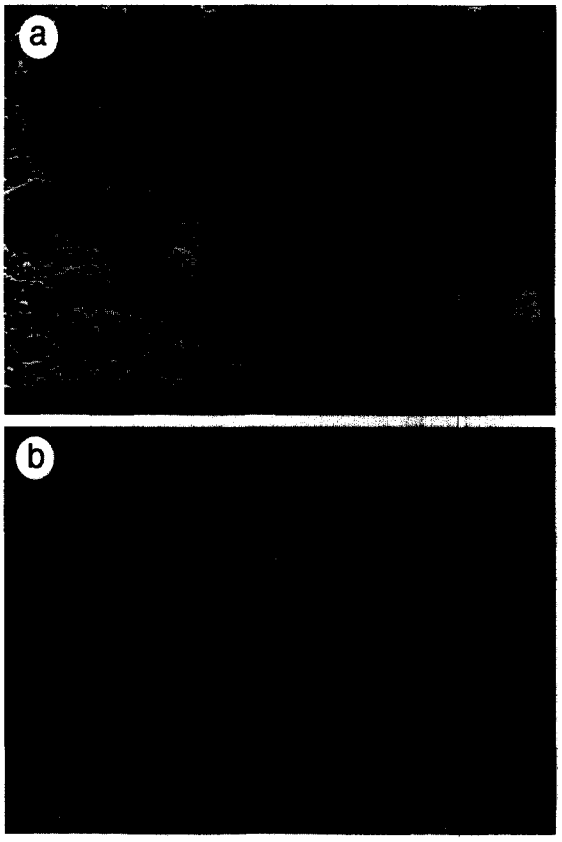

Fig. 7. (a) Morphology of VT50 catalyst (x 10000). (b) Isolated particle (x 20800).

are those that precipitate first. This conclusion was verified by analysis of the V/(V + Ti) ratios in the catalyst bulk and surface. In the sample VT10, the values of the V/(V + Ti) ratio are 0.89 in the bulk and 0.82 in the surface; this difference between bulk and surface concentration is in agreement with the fact that the vanadium phase precipitates first and then the titanium phase. In the catalyst VT90, the surface vanadium concentration V/(V + Ti) = 0.28 is higher than the bulk value V/(V + Ti) = 0.13.

The studies of several authors and the results of XRD analysis would indicate that solids VTiO are formed by a vanadium pentoxide phase that presents a large-sized plane (001) [7,24–26].

In the previous sections, it was established that catalysts VT10 and VT20 were composed

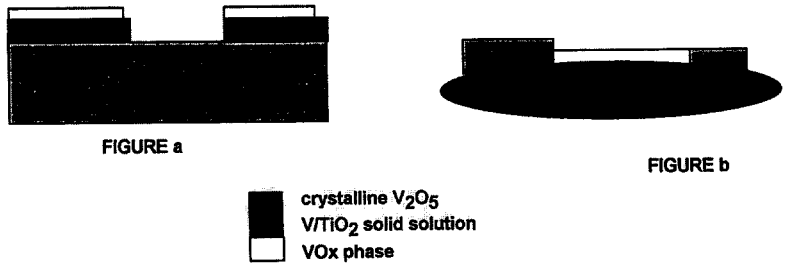

Fig. 8. (a) Particle Model of VT10 and VT20 catalysts. (b) Particle Model of VT50, VT80 and VT90 catalysts.

of crystalline V_2O_5 and vanadium in solid solution with TiO_2, covered by a monolayer of VOx species. Moreover, there may be pure TiO_2, i.e., that TiO_2 not substituted by vanadium atoms. On the basis of these data, we can propose the phase distribution of Fig. 8a in which the crystalline vanadium pentoxide, placed at the particle center, acts as support of solid solution particles covered by species VOx.

Unlike the previous ones, those catalysts having smaller V/Ti ratio (VT50, VT80 and VT90) are composed of much smaller round particles which, as formerly said, are typical of titanium dioxide. Such TiO_2 possess vanadium in solid solution, and is covered by species VOx. Besides, the XRD analysis indicated that the samples have crystalline V_2O_5 because of which the V/TiO_2 solid solution would act as a support of such crystals (Fig. 8b). As the size of these particles is smaller than those of VT10 and VT20, it is coherent to infer that the dimensions of the vanadium pentoxide crystals are smaller as well.

4. Conclusions

It was indicated in previous sections that the catalysts VTiO experience important morphological modifications as the titanium dioxide concentration increases. On the one hand, the shape of the particles varies from rectangular to circular owing to the gradual decrease in the concentration of V_2O_5 phase and the increase in TiO_2. On the other hand, and in parallel, we observed a size decrease, which is maximum in sample VT80.

These results and the different vanadium and titanium phases that compose coprecipitated VTiO catalysts, allowed us to propose a particle model of these solids. Those solids with a high vanadium content would have large crystalline V_2O_5 particles acting as a support of a V/TiO_2 solid solution covered by VOx species. Those solid with a high titanium content would have V/TiO_2 solid solution acting as a support of vanadium pentoxide.

The studies of several authors have demonstrated that by mixing oxides, doping oxides surface and varying the particle size, new acid sites are generated and the acid strength is changed [22,27,28]. This phenomenon is due to surface imperfections of the crystallographic structures in small particles; typical imperfections being metal or oxygen vacancies leading to a local charge imbalance. Such modifications of the acid–base properties has direct impact on the catalytic activity of the solids so it is important to consider here those studies dealing with methanol chemisorption on samples V_2O_5, VT10 and VT80 [29–31]. In such studies, the desorbed products were followed up as a function of time and temperature, and the results were that the samples of higher titanium content generated the typical products of methanol selective oxidation (formaldehyde, methyl formate, methylal, etc) more quickly and at lower temperature. The reaction mechanism involves first the adsorption of methanol on an acid site and then the partial oxidation to different species. In

summary, an increase in the acid strength of the adsorption site would favour reactant conversion and, as a consequence, could explain the increased activity in catalysts of smaller particle size.

References

[1] J. C. Volta and J. L. Portefaix, Appl. Catal., 18 (1985) 1.
[2] R. Saleh, I. Wachs, S. Chan and C. Chersich, J. Catal., 98 (1986) 102.
[3] G. Bond and S. Tahir, Appl. Catal., 71 (1991) 1.
[4] G. Deo, A. Turek, I. Wachs, N. Machej, H. Eckert and A. Hirt, Appl. Catal., A91 (1992) 27.
[5] C. Cristiani, P. Forzatti and G. Busca, J. Catal., 116 (1989) 586.
[6] F. Cavani, E. Foresti, F. Parrinello and F. Trifiró, Appl. Catal., 38 (1988) 311.
[7] J. Tatiboüet and J. Germain, C. R. Acad. Sc. Paris, 1983, t. 296, Serie II, p. 613.
[8] K. Mori, A. Miyamoto and Y. Murakami, Appl. Catal., 6 (1983) 213.
[9] J. Fierro, L. Arrua, J. Lopez Nieto and G. Kremenic, Appl. Catal., 37 (1988) 323.
[10] W.Slinkard and P. DeGroot, J. Catal., 68 (1981) 423.
[11] G. Busca, P. Tittarelli, E. Tronconi and P. Forzatti, J. Catal., 67 (1987) 91.
[12] F. Cavani, G. Genti, F. Parrinello and F. Trifiró, Stud. Surf. Sci. Catal., 31 (1987) 227.
[13] G. Centi, S. Perathoner and F. Trifiró, Res. Chem. Int., 15 (1991) 49.
[14] G. Centi, E.Giamello, D. Pinelli, and F. Trfiró, J. Catal., 130 (1991) 220.
[15] L. E. Briand, L. Gambaro and H. Thomas, J. Thermal An., 44 (1995) 803.
[16] L. Briand, L. Cornaglia, J. Güida and H. Thomas, J. Mater. Chem., 5 (1995) 1443.
[17] H. Viturro, C. Peez and R. Bonetto, Proc. IV Simposio Latinoamericano de Análisis por Técnicas de Rayos X, Chile, 1994.
[18] T. Seiyama, K. Nita, K. Maehara, N. Yamazoe and Y. Takita, J. Catal., 49 (1977) 164.
[19] R. Kozlowski, R. Pettifer and J. Thomas, J. Phys. Chem., 87 (1983) 5176.
[20] G. Went, L. Leu and A. Bell, J. Catal., 134 (1992) 479.
[21] E. J. Braunschweig, A. D. Logan, A. K. Datye and D. J. Smith, J. Catal., 118 (1989) 227.
[22] K. Nishiwaki, N. Kakuta, A. Ueno and H. Nakabayashi, J. Catal., 118 (1989) 498.
[23] M. Cabrera, O. Alfano and A. Cassano, Proc. IX Jornadas Argentinas de Catálisis, Argentina, 1995, p.381.
[24] A. Baiker and D. Monti, J. Catal., 91 (1985) 361.
[25] M. Gasior and T. Machej, J. Catal., 83 (1983) 472.
[26] D. Gasser and A. Baiker, J. Catal., 113 (1988) 325.
[27] C. L. Thomas, Ind. Eng. Chem., 41 (1949) 2564.
[28] K. Tanabe and T. Takeshida, Advances in Catalysis, Vol. 17, Academic Press, New York, 1967, p. 315.
[29] J. Sambeth, L. Gambaro and H. Thomas, Proc. XIV Simposio Iberoamericano de Catálisis, Vol. 2, p. 951, Chile, 1994.
[30] J. Sambeth, L. Gambaro and H. Thomas, J. Latin Am. Appl. Res., 24 (1994) 241.
[31] J. Sambeth, L. Gambaro and H. Thomas, Ads. Sc. and Tech., 12 (1995) 171. phase.